Electronic Supplementary Material (ESI) for ChemComm.

Supplementary Information

Increased CO_2 adsorption performance of chitosan derived activated carbons with nitrogen-doping

*Junpei Fujiki, Katsunori Yogo**

Chemical Research Group, Research Institute of Innovative Technology for the Earth (RITE),

9-2 Kizugawadai, Kizugawa, Kyoto 619-0292, Japan

*Corresponding Author: Katsunori Yogo

Phone: +81-774-75-2305, Fax: +81-774-75-2318, Email: yogo@rite.or.jp

Contents

Experimental

Characterization of prepared materials

The prepared NACs were characterized by N_2 adsorption–desorption at –196 °C on an ASAP 2420 automatic adsorption system (Micromeritics Instrument Co., Norcoss, GA). The specific surface area (S_{BET}) and pore size distribution were calculated using the Brunauer-Emmett-Teller (BET) and the non-localized density functional theory methods (slit pores), respectively. The S_{BET} was evaluated from adsorption data in an appropriate relative pressure range, which was selected to ensure that a positive intercept for multipoint BET fitting would be obtained. The micropore volume (V_{micro}) was obtained using a *t*-plot method (Harkins and Jura thickness equation) and compared with that calculated by Dubinin-Radushkevich equation. The total pore volume (V_{total}) was calculated from the amount of adsorbed N_2 at P/P_0=0.99. The average pore size was calculated using $4V_{total}/S_{BET}$. Scanning electron microscope and transmission electron microscope images of the prepared materials were obtained on a FE-SEM SU9000 (Hitachi High-Technologies Co., Tokyo, Japan) microscope and JEM-3100FEF (JEOL Ltd., Tokyo, Japan) microscope, respectively. The carbon structures of the prepared materials were analyzed by power X-ray diffraction measurements using a RINT2200 X-ray diffractometer (Rigaku Co., Tokyo, Japan). The nitrogen contents (N content) of the prepared materials were determined by elemental (CHN) analysis on a PE-2400 (Perkin Elmer, Waltham, MA).

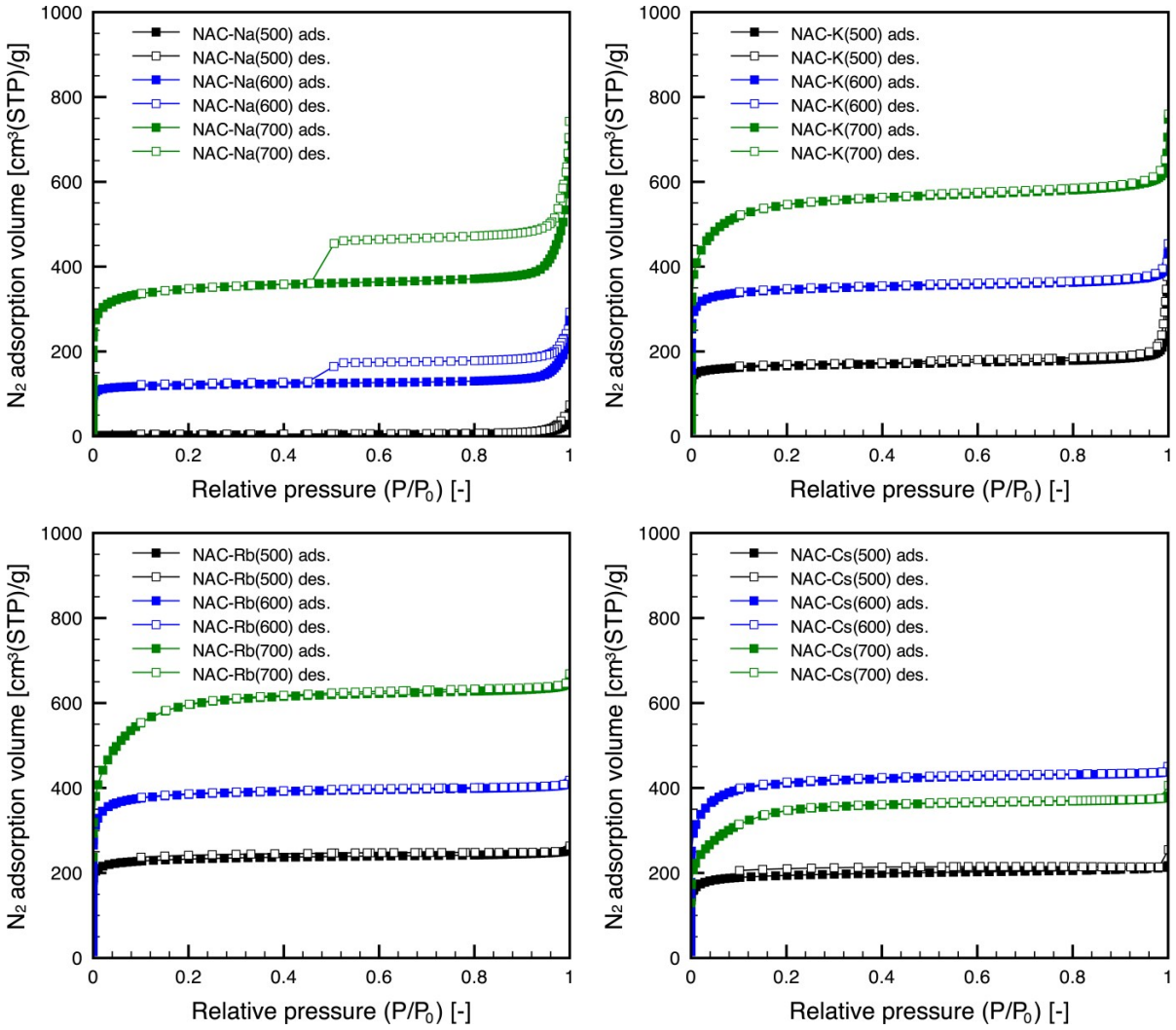

Figure S1 N_2 adsorption-desorption isotherms of the NACs at –196 °C.

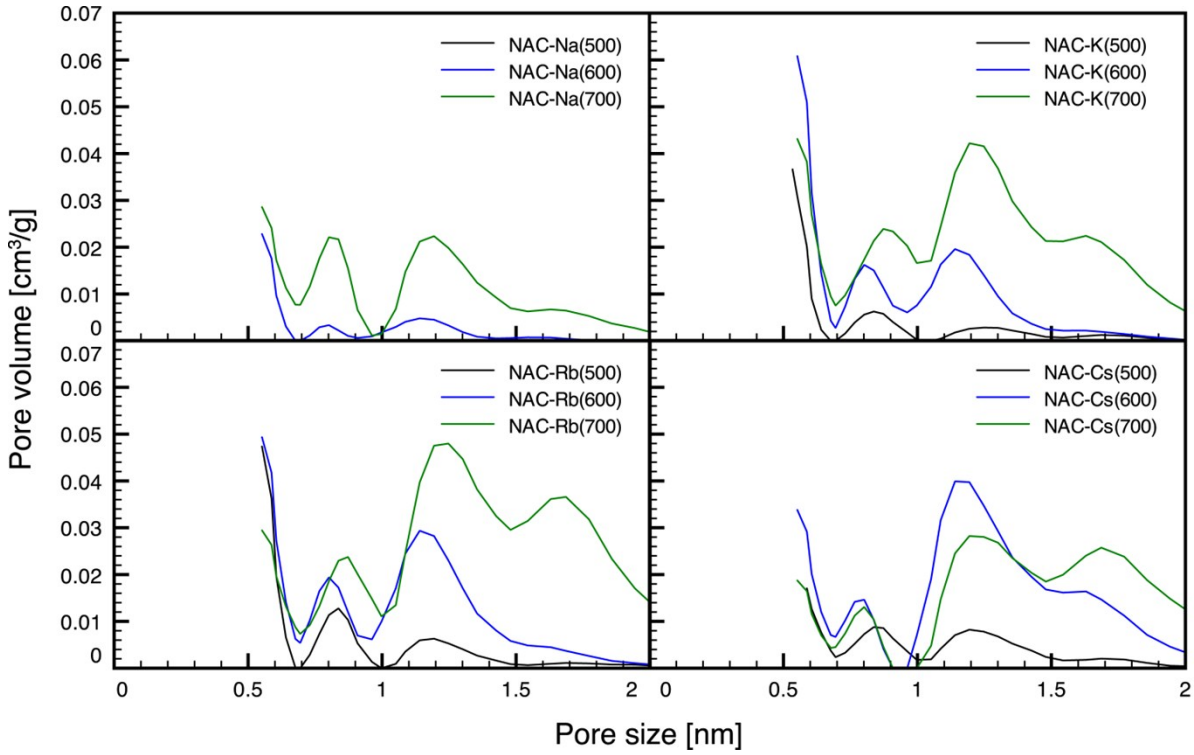

Figure S2 Pore size distributions of the NACs determined by the non-localized density functional theory method.

Table S1 Comparison of micropore volumes of the NACs determined by the t-plot method and the Dubinin-Radushkevich equation (D-R eq.).

	V_{micro} [cm^3/g]		Average pore size ($4V_{total}/S_{BET}$) [nm]
	t-plot	D-R eq.	
NAC-Na(500)	0.00	0.00	15.44
NAC-K(500)	0.22	0.25	2.10
NAC-Rb(500)	0.30	0.34	1.66
NAC-Cs(500)	0.22	0.25	1.80
NAC-Na(600)	0.16	0.18	2.67
NAC-K(600)	0.47	0.53	1.77
NAC-Rb(600)	0.52	0.59	1.69
NAC-Cs(600)	0.50	0.61	1.77
NAC-Na(700)	0.43	0.52	2.35
NAC-K(700)	0.62	0.78	1.88
NAC-Rb(700)	0.55	0.81	1.85
NAC-Cs(700)	0.26	0.47	1.88

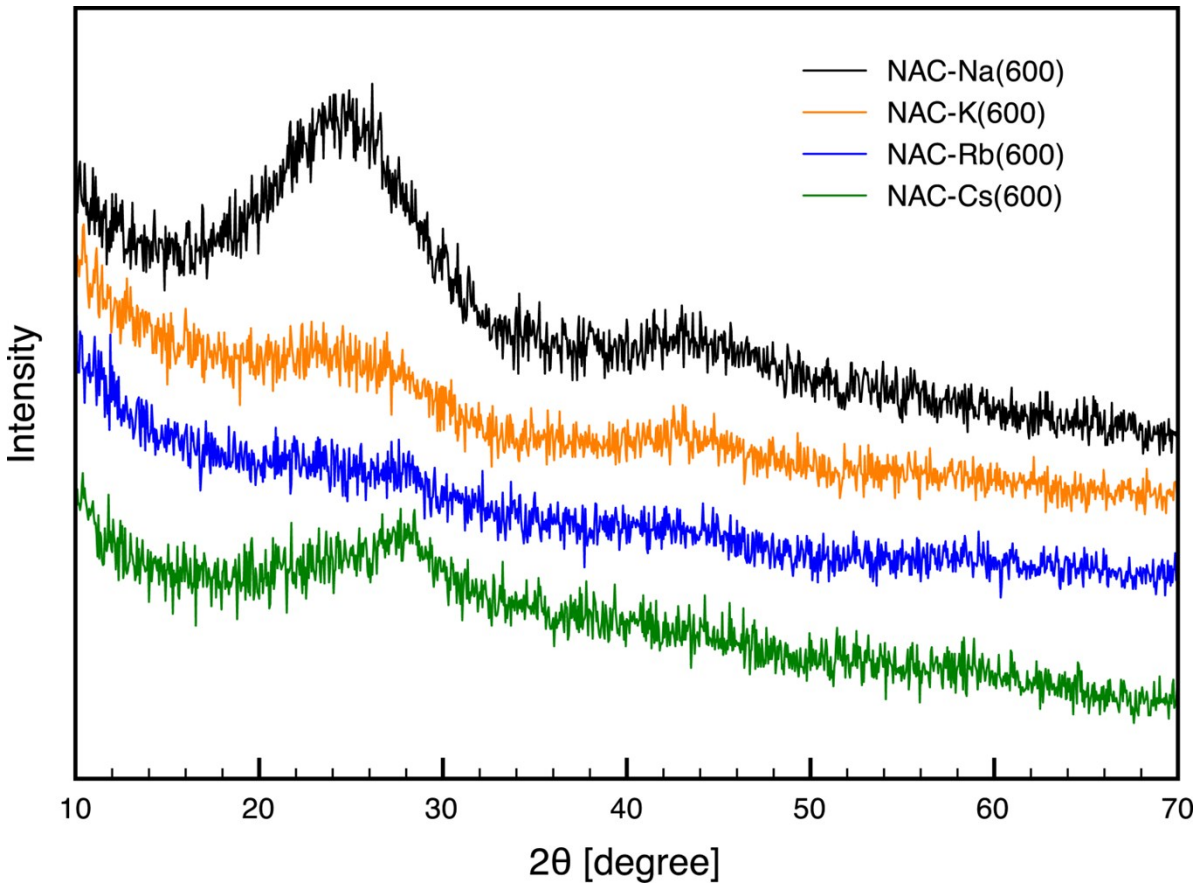

Figure S3 Powder X-ray diffraction pattern of NAC-M(600).

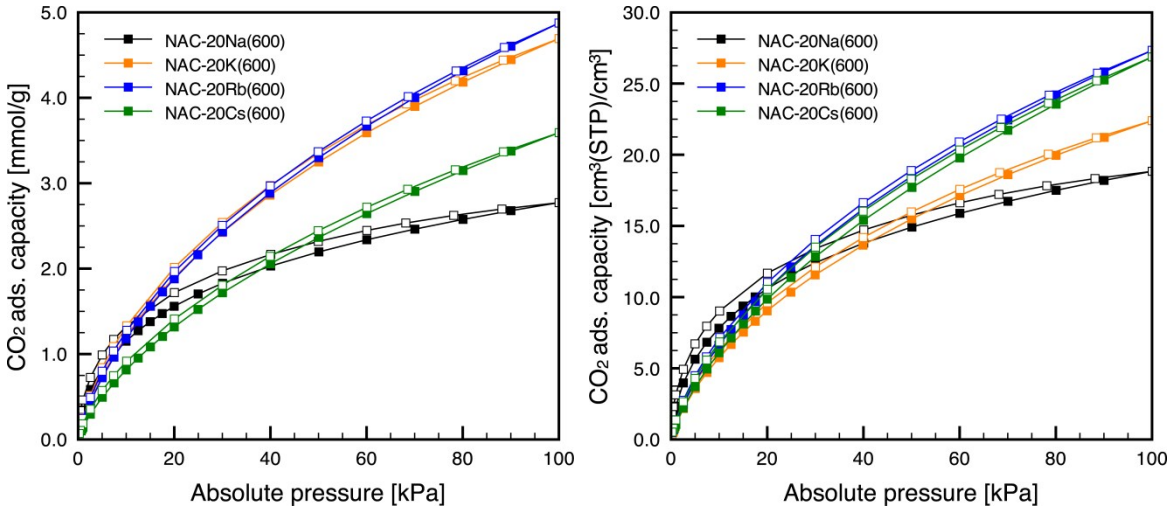

Figure S4 Gravimetric and volumetric CO_2 adsorption capacities of NAC-*M*(600) at 25 ˚C, considering bulk densities of NAC-Na(600), NAC-K(600), NAC-Rb(600) and NAC-Cs(600) to be 0.303, 0.213, 0.250 and 0.334 g/cm^3, respectively).

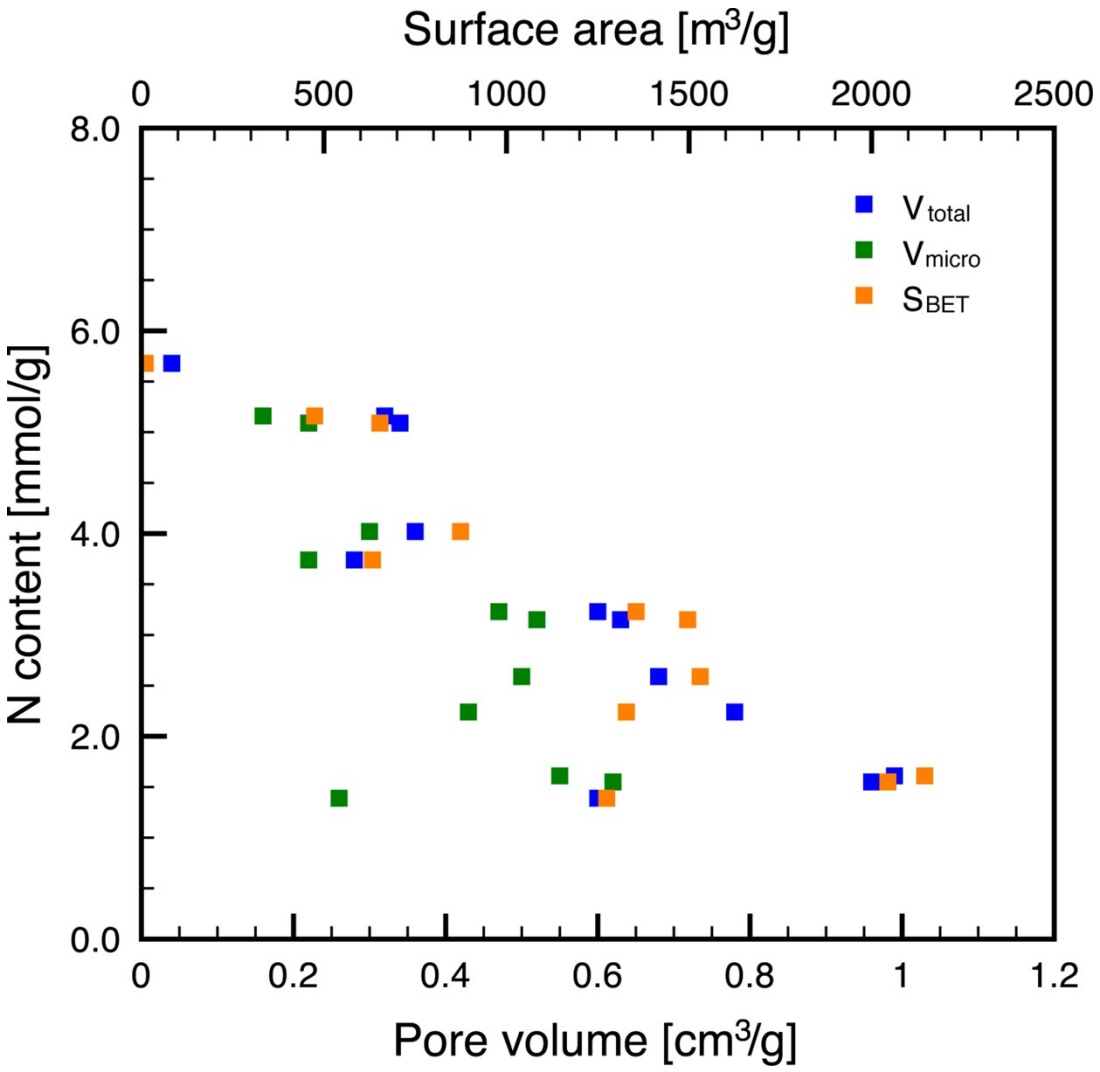

Figure S5 Relationship between N content, pore volume and surface area for the NACs.

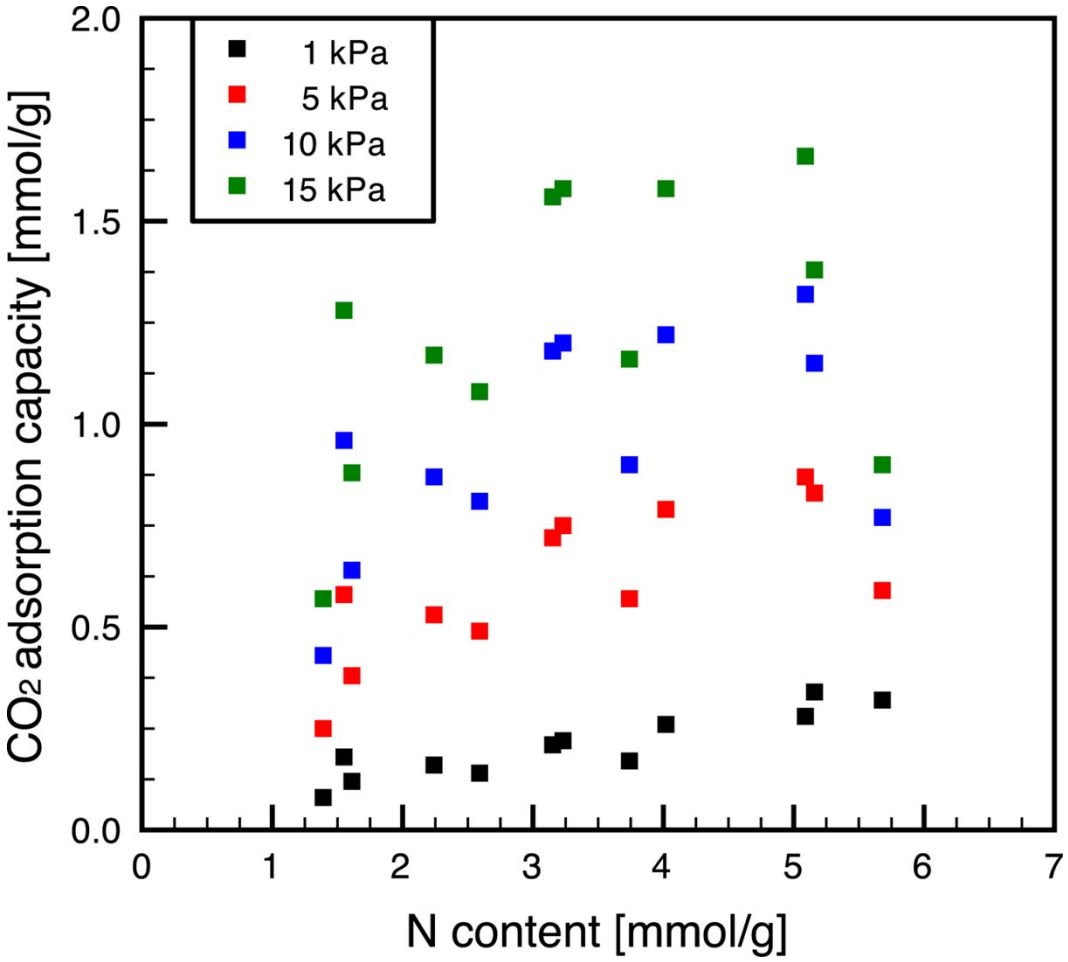

Figure S6 Relationship between N content and CO_2 capacity at 1, 5, 10 and 15 kPa.